Science and Technology Indonesia
e-ISSN:2580-4391 *p*-ISSN:2580-4405
Vol. 9, No. 1, January 2024

Research Paper

Preissmann Four-Point Methods for Solution of Simplified Saint-Venant Equations Applied to Flood Routing in Prismatic Open Channels

Bambang Agus Sulistyono[1*], Suryo Widodo[1]

[1]*Department of Mathematics Education, Faculty of Health and Science, University of Nusantara PGRI Kediri, Kediri, 64112, Indonesia*
***Corresponding author**: bb7agus1@unpkediri.ac.id*

Abstract
This research goal to compare the flow properties in the rectangular and trapezoidal open channels by examining the influence of the channel side slope is depicted by simplified Saint-Venant Equations. The solution of these equations has been completed numerically by using Preissmann four-point scheme. The model is simulated using the Matlab application to point out the flow properties. The proposed model is validated by the model without simplification which was selected from the literature. The validation outcomes indicate that in common, the simulation outcomes of the two models have a good agreement. The simulation results show that the greater the slope of the channel side, the greater the peak discharge and the greater the time shift. The analysis emphasizes how channel geometry influences flow behavior, indicating that trapezoidal channels, with inclined side slopes z, yield slightly higher peak discharges compared to rectangular ones. For $z = 0$, discharge of peak $Q = 7.38$ m^3/s and $t = 18$ s. For $z = 2$, discharge of peak $Q = 7.39$ m^3/s and $t = 21$ s. For $z = 4$, discharge of peak $Q = 7.45$ m^3/s and $t = 23$ s. For $z = 6$, discharge of peak $Q = 7.51$ m^3/s and $t = 24$ s.

Keywords
Prismatic Channel Flow, Simplified Saint-Venant Equations, Preissmann Four-Point Scheme, Flow Properties

Received: 7 July 2023, Accepted: 14 January 2024
https://doi.org/10.26554/sti.2024.9.1.183-188

1. INTRODUCTION

A flood is an affair that is caused by the rise of the water stage to exceed the volume of water reservoirs such as rivers or waterways. Floods may be forecasted by viewing natural phenomena such as aloft rainfall. (Mandailing et al., 2020; Piadeh et al., 2022; Sulistyono and Wiryanto, 2018). The event of flooding is complicated to forecast if it comes flashy. Floods shall induce troubles and disadvantages such as damage to objects, electronic equipment, machines, securities, etc. The negative impact of the flood may damage houses, buildings, and bridges, and can cut off transportation means, so forecasting is needed as an early warning of flooding.

Unsteady flow is a flow feature that is often found in rivers and waterways (Sulistyono et al., 2021a). For planning, flood control, maintenance, and other work-related drains, mathematical models have played an important role in various disciplines of fluid mechanics, whether in research, engineering, or industry. Not to forget, in the field of hydraulics, a mathematical model is increasingly showing its existence as indicated by the increasing frequency of mathematical models used in engineering work, in the study and design stages. In forecasting floods in natural or artificial channels, three major factors influence the outcomes of numerical simulations (Keskin, 1970; Sulistyono and Wiryanto, 2017) namely, the mathematical model that depicts the water flow movement, the numerical scheme used to resolve the mathematical model, and the characteristics of the channel.

The Saint-Venant equations are a mathematical model quite reliable for depicting the behavior flow of a flood in a natural as well as an artificial channel (Pudjaprasetya, 2018). This model is system differential partial nonlinear and complex, so analytical solutions are available only for special cases. Therefore, some researchers make simplifications and modifications to the model such as the kinematic wave equation (Krutov et al., 2021; Moramarco et al., 2008; Ogunlela and Adelodun, 2014; Zheng et al., 2020), diffusive wave equation (Jahanbazi et al., 2017; Moussa and Majdalani, 2021; Wang et al., 2003; Wu et al., 2019), inertia dynamic wave equation (Cozzolino et al., 2019). On the contrary, the Saint-Venant equations, in their complete form, have been addressed using diverse numerical methods for both cylindrical and non-uniformly shaped cross-sections. These established solutions, as documented by (Amien and Fang, 1970; Koussis, 1976; Lamberti and Pilati, 1996; Sulistyono and Wiryanto, 2019; Mirzazadeh and

Akbari, 2023), are presently in use. Yet, the majority of these solutions demand substantial computational resources and time investment.

In this study, we used a simplified model by modifying the momentum equation. This occurs because modifications to the Saint-Venant equations will decrease the required boundary conditions and save computational time. The simplified model will be solved numerically using too a simple numerical method, namely the implicit finite difference method, often called the four-point Preissmann method. The cross-sectional configuration of the channel is a crucial characteristic of prismatic channels. The cross-section of a natural channel is frequently intricate or complex (Komi et al., 2017; Kandpal and Bora, 2023). Hence, it's crucial to transform its complex cross-section into a simpler form that exhibits a comparable hydraulic response in mathematical modeling (Ficchì et al., 2019; Paprotny et al., 2020; Neira et al., 2020). Depending on the complexity of their cross-sections, artificial and natural channels may be represented by a blend of four basic geometric elements: triangular, semi-circular, rectangular, or trapezoidal shapes. We select rectangular and trapezoidal cross-sections because they are the most widely used in the field (Pu et al., 2020). In this research, we will compare the flow properties in the rectangular and trapezoidal open channels by examining the influence of the channel side slope.

2. EXPERIMENTAL SECTION

2.1 Simplified Saint Venant Equations

The behavior of a one-dimensional unsteady water flow in an open channel can often be depicted using a mathematical model known as the Saint-Venant's equations (Chaudhry, 2008) as follows,

$$\frac{\partial A}{\partial t} + \frac{\partial Q}{\partial x} = 0 \tag{1}$$

$$\frac{\partial Q}{\partial t} + \frac{\partial}{\partial x}\left(\frac{Q^2}{A}\right) + gA\left(\frac{\partial h}{\partial x} - S_0\right) + gAS_f = 0 \tag{2}$$

here, A states the area of cross-sectional wet, Q states the discharge, g states the acceleration of gravity, h states the flow depth, S_0 states the channel bottom slope, and S_0 states the slope of friction slope, x states space co-ordinate and t states time.

The simplified Saint Venant's equations for rectangular cross-section and trapezoidal cross-section are obtained by transforming Equation (2) into an equation of partial differential which only has two parameters of discharge and wet cross-sectional area.

2.2 Rectangular Cross-Section

For flood routing in the rectangular cross-section in Figure 1, The area of the cross-section can be expressed as

$$A = bh \tag{3}$$

In this context, b signifies the width of the channel.

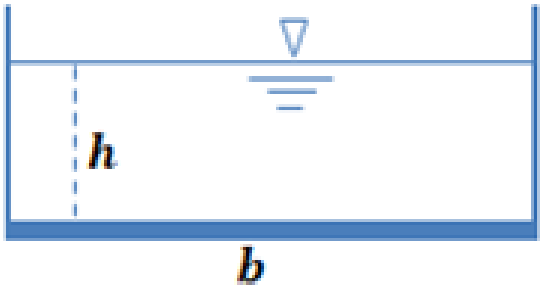

Figure 1. Rectangular Cross-Section

Assuming a constant channel width, Equation (2) is simplified to an equation that only applies to rectangular cross-sections (Geravand et al., 2020; Sulistyono et al., 2021b), i.e.

$$\frac{\partial Q}{\partial t} + \alpha\frac{\partial Q}{\partial x} + \beta = 0 \tag{4}$$

in which

$$\alpha = 2\frac{Q}{A} + \frac{\frac{gA}{b} - \frac{Q^2}{A^2}}{\frac{Q}{A}\left(\frac{5}{3} - \frac{4}{3}\frac{R}{b}\right)} \tag{5}$$

and

$$\beta = gA\left(\frac{Q^2 n^2}{A^2 R^{4/3}} - S_0\right) \tag{6}$$

Hence, Equation (4) can be resolved utilizing the Preissmann four-point scheme that satisfies both initial and boundary conditions. In flood routing, the inflow hydrograph can accommodate various geometrical configurations.

2.3 Trapezoidal Cross-Section

For flood routing in trapezoidal cross-section in Figure 2, The expression for the cross-sectional area is given by

$$A = (b + zh)h \tag{7}$$

where *bis* width of the channel and z is the side channel slope. Assuming the channel width remains constant, Equation (2) is simplified to an equation that only applies to trapezoidal cross-section (Sulistyono and Wiryanto, 2017) i.e.

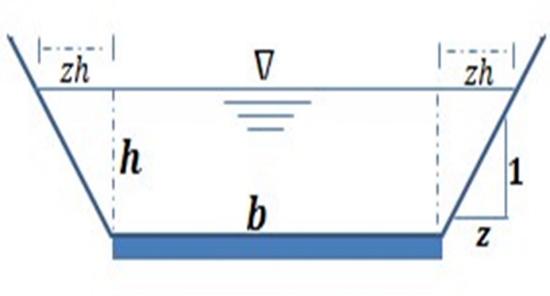

Figure 2. The Cross-Section of Trapezium

$$\frac{\partial Q}{\partial t} + \alpha \frac{\partial Q}{\partial x} + \beta = 0 \tag{8}$$

in which

$$\alpha = 2\frac{Q}{A} + \frac{\frac{gbA}{(b^2+2zA)} - \frac{Q^2}{A^2}}{\frac{Q}{A}\left(\frac{5}{3} - \frac{4}{3}\frac{bR\sqrt{1+z^2}}{(b^2+2zA)}\right)} \tag{9}$$

and

$$\beta = gA\left(\frac{Q^2 n^2}{A^2 R^{4/3}} - S_0\right) \tag{10}$$

Hence, Equation (8) can be resolved utilizing the Preissmann four-point scheme that satisfies both initial and boundary conditions. In flood routing, the inflow hydrograph can accommodate various geometrical configurations.

2.4 Numerical Schemes

In order to resolve the simplified Saint-Venant equations, a Preissmann four-point finite difference method is applied to get the numerical solutions. In this scheme, the time derivatives are approached by a forward difference operator centered between the i^{th} and $i+1$ points along the x-axis as follow

$$\frac{\partial f}{\partial t} = \frac{f_i^{j+1} - f_{i-1}^{j+1} + f_i^j - f_{i-1}^j}{2\Delta x} \tag{11}$$

Where fdenotes any variable. The spatial derivatives are approached by a forward difference operator positioned between two neighboring time steps corresponding to weighting factors of θ and 1-θ as follow

$$\frac{\partial f}{\partial x} = \theta\left(\frac{f_i^{j+1} - f_{i-1}^{j+1}}{\Delta x}\right) + (1-\theta)\left(\frac{f_i^j - f_{i-1}^j}{\Delta x}\right) \tag{12}$$

thus,

$$f = \theta\left(\frac{f_i^{j+1} + f_{i-1}^{j+1}}{2}\right) + (1-\theta)\left(\frac{f_i^j + f_{i-1}^j}{2}\right) \tag{13}$$

Futhermore, substitute Equations (11) and (12) into Equations (1) and (4), we get

$$Q_i^{j+1} = C_1 Q_{i-1}^j + C_2 Q_i^j + C_3 Q_{i-1}^{j+1} - C_4 \beta_i^j \tag{14}$$

$$A_i^{j+1} = A_{i-1}^j + A_i^j - A_{i-1}^{j+1} - \frac{2\Delta t}{\Delta x}\left[\theta\left(Q_i^{j+1} - Q_{i-1}^{j+1}\right) + (1-\theta)\left(Q_i^j - Q_{i-1}^j\right)\right] \tag{15}$$

where

$$C_1 = \frac{\Delta x + 2\Delta t\alpha(1-\theta)}{\Delta x + 2\Delta t\theta\alpha} \tag{16}$$

$$C_2 = \frac{\Delta x - 2\Delta t\alpha(1-\theta)}{\Delta x + 2\Delta t\theta\alpha} \tag{17}$$

$$C_3 = \frac{2\Delta t\theta\alpha - \Delta x}{\Delta x + 2\Delta t\theta\alpha} \tag{18}$$

$$C_4 = \frac{2\Delta t\Delta x}{\Delta x + 2\Delta t\theta\alpha} \tag{19}$$

in which

$$\beta_i^j = gA_i^j\left(\frac{n^2(Q_i^j)^2}{(A_i^j)^2(R_i^j)^{4/3}}\right) \tag{20}$$

$$\alpha_i^j = 2\frac{Q_i^j}{A_i^j} + \left(\frac{\frac{gA_i^j}{b} - \frac{(Q_i^j)^2}{(A_i^j)^2}}{\frac{Q_i^j}{A_i^j}\left(\frac{5}{3} - \frac{4}{3}\frac{R_i^j}{b}\right)}\right) \text{for rectangular channel} \tag{21}$$

$$\alpha_i^j = 2\frac{Q_i^j}{A_i^j} + \left(\frac{\frac{gbA_i^j}{b^2+2zA_i^j} - \frac{Q_i^j}{A_i^j}}{\frac{Q_i^j}{A_i^j}\left(\frac{5}{3} - \frac{4}{3}\frac{bR_i^j\sqrt{1+z^2}}{b^2+2zA_i^j}\right)}\right) \text{for trapezoidal channel} \tag{22}$$

It's evident that each set of values for α_i^j and β_i^j can be easily computed from Equation (20), Equation (21) for rectangular cross-section, and Equation (22) for trapezoidal cross-section, utilizing the available initial and boundary data at the starting

point of (i, j). This allows for determining Q_i^{j+1} from Equation (14). Ultimately, with Q_i^{j+1} established, A_i^{j+1} can be calculated using Equation (15). This procedure will be reiterated for successive (i, j) values.

To ensure the proposed numerical method can be used for simulation, it's crucial to validate the scheme. The proposed model is validated with model without simplification in rectangular channel (Sulistyono and Wiryanto, 2019). The validation results, as shown in Figure 3, suggest that overall, the simulation results from both models are well-matched. Minor discrepancies arise due to the simplifications considered in the proposed model.

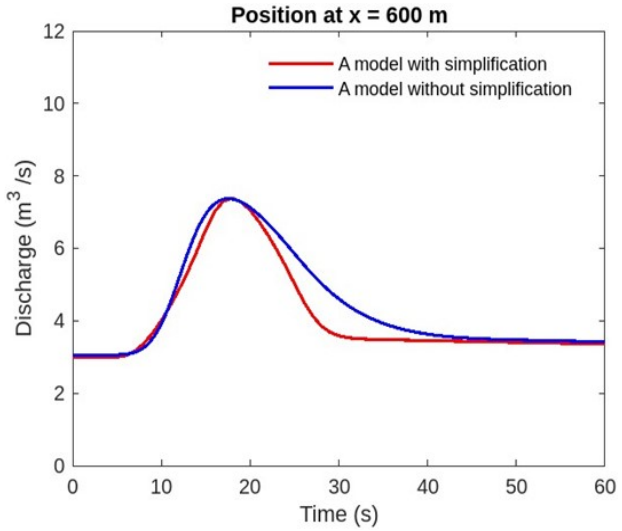

Figure 3. Discharge from the Model without Simplification and the Model with Simplification at Position $x = 600$m

3. RESULTS AND DISCUSSION

Water flows from upstream through a prismatic channel featuring both rectangular and trapezoidal cross-sections. From the upstream direction, it is recorded that the inflow hydrograph in the form of a triangular enters the channel with the following data:

$$Q(0,t) = \begin{cases} 3 + 0.9t & \text{for } 0 \le t < 10 \\ 12 - 0.9(t-10) & \text{for } 10 \le t < 20 \\ 3 & \text{for } t \ge 20 \end{cases} \quad (23)$$

with the initial coditions are $Q(x, 0) = 3$ m ^{3}/s and $A(x, 0) = 3$ m^2. The fundamental elements utilized in numerical simulations include: length of channel $L = 2000$ m, constant width of the channel $b = 5$ m, the bottom slope of the channel $S_0 = 0.0005$, roughness coefficient of Manning $n = 0.0138$, gravity acceleration $g = 9.81$ m/s^2, spatial step 100 m, time step $t = 10$s, and the The simulation runs for $t = 50$ s.

The simplified Saint-Venant equations developed in this study were applied to perform several simulations, under identical initial and boundary conditions, by evaluating wave propagation along a channel with rectangular and trapezoidal cross-sections, as follows.

3.1 Outflow Hydrograph in Rectangular and Trapezoidal for $z = 0$

In order to ensure that the derivation of the trapezoidal channel formula is valid, the following simulation will display the outflow hydrograph that occurs in rectangular and trapezoidal cross-sections at $z = 0$. Figure 4 displays the outflow hydrograph, observed 600 meters downstream, derived from a triangular inflow hydrograph. It's noticeable that the peak discharge has reduced from 12 m^3/s to 7.38 m^3/s and The peak discharge time has shifted from 10 s to 18 s. It can be seen that the outflow hydrograph profile of the rectangular channel and trapezoidal cross-section for $z = 0$ has very high suitability. This result confirms to us that the trapezoidal cross-sectional channel formula is valid.

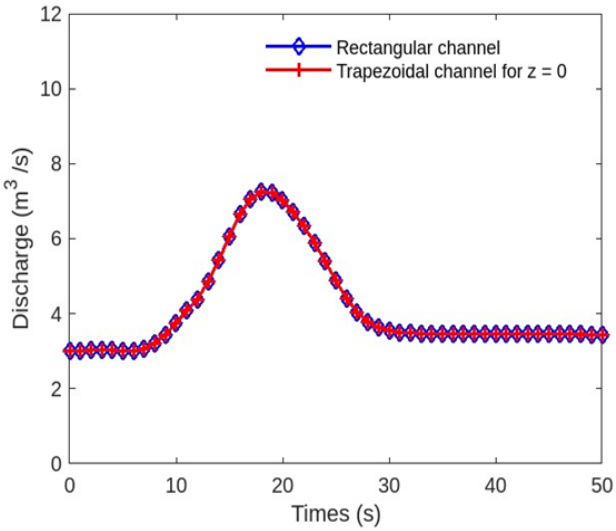

Figure 4. Profile Discharge in Rectangular and Trapezoidal for $z = 0$

3.2 Outflow Hydrograph in Rectangular and Trapezoidal

In this section, simulations are performed to compare behavior flows at a trapezoidal channel with a rectangular channel. This study involves simulating the movement of water through prismatic channels in response to a triangular hydrograph inflow. The focus is on examining how water discharge behaves 600 meters downstream from the initial point. Two channel cross-sections, rectangular and trapezoidal, with different side slopes are being analyzed. Figure 5 illustrates an increasing trend in both the peak of the hydrograph and the z value. The specific values for peak discharge and corresponding time intervals are provided for different scenarios (perhaps different configurations or conditions) under investigation. These values help

assess the variations in water flow and discharge characteristics in the channel under distinct circumstances.

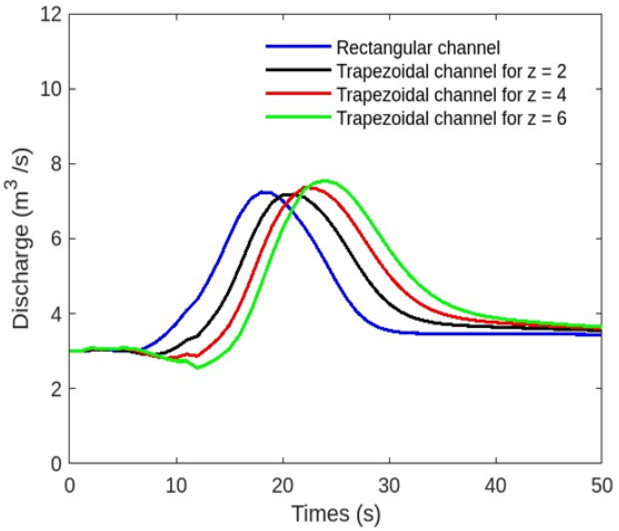

Figure 5. Compare discharge in rectangular and trapezoidal for $z = 2$, $z = 4$, $z = 6$

Simulation of routing water flows in prismatic channels due to hydrograph inflow triangular. Furthermore, observations were made on the discharge behavior at a location 600 m from the upstream. There are two cross-sections of the channel being reviewed, namely rectangular cross-section and trapezoidal cross-section for the larger side slope. Figure 5 it can be seen that the peak of the hydrograph is getting bigger and the value of z is getting bigger as well. For $z = 0$, the peak of discharge $Q = 7.38$ m^3/s and $t = 18$ s. For $z = 2$, the peak of discharge $Q = 7.39$ m^3/s and $t = 21$ s. For $z = 4$, the peak of discharge $Q = 7.45$ m^3/s and $t = 23$ s. For $z = 6$, the peak of discharge $Q = 7.51$ m^3/s and $t = 24$ s.

4. CONCLUSION

To compute flood routing in rectangular and trapezoidal channels, the study introduced simplified Saint-Venant equations and the Preissmann four-point scheme. The results obtained from the model in the trapezoidal channel are compared with those in the rectangular channel, both under identical conditions. The results suggest that as the slope of the channel side increases, both the peak discharge and the time shift also increase. Following this comparative analysis, it becomes evident that in the case of the trapezoidal channel, there's a substantial increase in peak flow discharge compared to the rectangular channel with identical side slopes. Furthermore, a more pronounced time shift is also observed in the trapezoidal channel, emphasizing the significant role of channel geometry in flood flow modeling. This underscores the necessity to account for channel shape in predicting flood flow characteristics more accurately, especially considering its impact on peak discharge and temporal aspects of the flow.

5. ACKNOWLEDGEMENT

The researchers extend their gratitude to LPPM Nusantara University PGRI Kediri for their support of this research via the University's 2023 Research Stimulus Program.

REFERENCES

Amien, M. and C. Fang (1970). Implicit Flood Routing in Channel Network. *Journal Hydraulic Division, ASCE*, **96**; 918–926

Chaudhry, M. H. (2008). *Open-Channel Flow*, volume 523. Springer

Cozzolino, L., L. Cimorelli, R. Della Morte, G. Pugliano, V. Piscopo, and D. Pianese (2019). Flood Propagation Modeling with the Local Inertia Approximation: Theoretical and Numerical Analysis of Its Physical Limitations. *Advances in Water Resources*, **133**(2); 103422

Ficchì, A., C. Perrin, and V. Andréassian (2019). Hydrological Modelling at Multiple Sub-Daily Time Steps: Model Improvement Via Flux-Matching. *Journal of Hydrology*, **575**; 1308–1327

Geravand, F., S. M. Hosseini, and B. Ataie-Ashtiani (2020). Influence of River Cross-Section Data Resolution on Flood Inundation Modeling: Case Study of Kashkan River Basin in Western Iran. *Journal of Hydrology*, **584**(2); 124743

Jahanbazi, M., I. Özgen, R. Aleixo, and R. Hinkelmann (2017). Development of a Diffusive Wave Shallow Water Model with a Novel Stability Condition and Other New Features. *Journal of Hydroinformatics*, **19**(3); 405–425

Kandpal, S. and S. N. Bora (2023). Analytical Solution for Linearized Saint-Venant Equations with a Uniformly Distributed Lateral Inflow in a Finite Rectangular Channel. *Water Resources Management*, **37**(14); 5655–5676

Keskin, M. (1970). A Model of Free Surface Flow for Prismatic Channels. *WIT Transactions on Modelling and Simulation*, **24**; 121–127

Komi, K., J. Neal, M. A. Trigg, and B. Diekkrüger (2017). Modelling of Flood Hazard Extent in Data Sparse Areas: A Case Study of the Oti River Basin, West Africa. *Journal of Hydrology: Regional Studies*, **10**; 122–132

Koussis, A. (1976). An Approximate Dynamic Flood Routing Method. In *Int. Symposium on Unsteady Flow in Open Channel*. Univ. of Newcastle-upon-Tyne

Krutov, A., R. Choriev, B. Norkulov, D. Mavlyanova, and A. Shomurodov (2021). Mathematical Modelling of Bottom Deformations in the Kinematic Wave Approximation. In *IOP Conference Series: Materials Science and Engineering*, volume 1030. IOP Publishing, page 012147

Lamberti, P. and S. Pilati (1996). Flood Propagation Models for Real-Time Forecasting. *Journal of Hydrology*, **175**(1-4); 239–265

Mandailing, P. M., W. Mardiansyah, M. Irfan, A. Arsali, and I. Iskandar (2020). Characteristics of Diurnal Rainfall Over Peatland Area of South Sumatra, Indonesia. *Science and Technology Indonesia*, **5**(4); 136–141

Mirzazadeh, P. and G. H. Akbari (2023). Flood Wave Simulation Case Study for Natural Water Stream by Numerical Solutions of Unsteady Equations. *Journal of Hydrosciences and Environment*, **6**(11); 1–8

Moramarco, T., C. Pandolfo, and V. P. Singh (2008). Accuracy of Kinematic Wave Approximation for Flood Routing. II. Unsteady Analysis. *Journal of Hydrologic Engineering*, **13**(11); 1089–1096

Moussa, R. and S. Majdalani (2021). Use of the Hayami Diffusive Wave Equation to Model the Relationship Infected–Recoveries–Deaths of Covid-19 Pandemic. *Epidemiology & Infection*, **149**; 1–13

Neira, J. M. T., G. Tallec, V. Andréassian, and J. Mouchel (2020). A Combined Mixing Model for High-Frequency Concentration–Discharge Relationships. *Journal of Hydrology*, **591**; 125559

Ogunlela, A. and B. Adelodun (2014). Kinematic Parameters for Asa River Routing. *International Journal of Environmental and Ecological Engineering*, **8**(5); 346–350

Paprotny, D., H. Kreibich, O. Morales-Nápoles, A. Castellarin, F. Carisi, and K. Schröter (2020). Exposure and Vulnerability Estimation for Modelling Flood Losses to Commercial Assets in Europe. *Science of the Total Environment*, **737**; 140011

Piadeh, F., K. Behzadian, and A. M. Alani (2022). A Critical Review of Real-Time Modelling of Flood Forecasting in Urban Drainage Systems. *Journal of Hydrology*, **607**(12); 1–16

Pu, J. H., M. Pandey, and P. R. Hanmaiahgari (2020). Analytical Modelling of Sidewall Turbulence Effect on Streamwise Velocity Profile Using 2D Approach: A Comparison of Rectangular and Trapezoidal Open Channel Flows. *Journal of Hydro-Environment Research*, **32**; 17–25

Pudjaprasetya, S. R. (2018). *Transport Phenomena, Equations and Numerical Methods*. INA-Rxiv

Sulistyono, B. A., S. Samijo, N. Aan, D. D. Yohanie, and A. D. Handayani (2021a). Numerical Simulation of Flood Routing through Channels with Area Variation using Staggered Grid Method. *Science and Technology Indonesia*, **6**(4); 261–266

Sulistyono, B. A., S. Samijo, and D. D. Yohanie (2021b). Numerical Simulation of Flood Routing using the Simplified Saint Venant Equations in Rectangular Channels. *Indonesian Journal of Pure and Applied Mathematics*, **3**(2); 63–74

Sulistyono, B. A. and L. Wiryanto (2017). Investigation of Flood Routing by a Dynamic Wave Model in Trapezoidal Channels. In *AIP Conference Proceedings*, volume 1867. AIP Publishing

Sulistyono, B. A. and L. Wiryanto (2018). An Analysis of the Influence of Variability Rainfall on Flow Rate Based on the Watershed Characteristics. In *IOP Conference Series: Earth and Environmental Science*, volume 124. IOP Publishing, page 012001

Sulistyono, B. A. and L. H. Wiryanto (2019). A Staggered Method for Numerical Flood Routing in Rectangular Channels. *Advances and Applications in Fluid Mechanics*, **23**(2); 171–179

Wang, G., S. Chen, J. Boll, and V. Singh (2003). Nonlinear Convection-Diffusion Equation with Mixing-Cell Method for Channel Flood Routing. *Journal of Hydrologic Engineering*, **8**(5); 259–265

Wu, H., P. Fu, J. P. Morris, R. R. Settgast, and F. J. Ryerson (2019). ICAT: A Numerical Scheme to Minimize Numerical Diffusion in Advection-Dispersion Modeling and Its Application in Identifying Flow Channeling. *Advances in Water Resources*, **134**; 103434

Zheng, H., E. Huang, and M. Luo (2020). Applicability of Kinematic Wave Model for Flood Routing under Unsteady Inflow. *Water*, **12**(9); 2528

